Instructions for use

One-Shot Intrablock Crosslinking of Linear Diblock Copolymer to Realize Janus-shaped Single-Chain Nanoparticle

Kodai Watanabe,[a] Noya Kaizawa,[a] Brian J. Ree,[b] Takuya Yamamoto,[b] Kenji Tajima,[b]

Takuya Isono,*,[b] Toshifumi Satoh*,[b]

[a] Dr. K. Watanabe, Mr. N. Kaizawa
Graduate School of Chemical Sciences and Engineering, Hokkaido University, Sapporo 060-8628, Japan
[b] Prof. B. J. Ree, Prof. T. Yamamoto, Prof. K. Tajima, Prof. T. Isono,* Prof. T. Satoh*
Faculty of Engineering, Hokkaido University, Sapporo 060-8628, Japan
E-mail: isono.t@eng.hokudai.ac.jp (T. Isono); satoh@eng.hokudai.ac.jp (T. Satoh)

Supporting information for this article is given via a link at the end of the document.

Abstract: Developing an efficient and versatile process to transform a single linear polymer chain into a shape-defined nanoobject is a major challenge in the fields of chemistry and nanotechnology to replicate sophisticated biological functions of proteins and nucleic acids in a synthetic polymer system. In this study, we performed one-shot intrablock crosslinking of linear block copolymers (BCPs) to realize single-chain nanoparticles (SCNPs) with two chemically compartmentalized domains (i.e., Janus-shaped SCNPs). Detailed structural characterizations of the Janus-shaped SCNP composed of polystyrene-*block*-poly(glycolic acid) revealed its compactly folded conformation and compartmentalized block localization, similar to the self-folded tertiary structures of natural proteins. Versatility of the one-shot intrablock crosslinking was demonstrated using several different BCP precursors. We further discovered the excellent self-assembling behavior of the Janus-shaped SCNP to produce miniscule microphase-separated structures, representing the significant potential of the presented compartmentalization protocol,
for developing biomimetic synthetic-systems, as well as for industrial nanofabrication applications.

Introduction

Inspired by the self-folding of biomacromolecules, such as proteins and nucleic acids, intramolecular crosslinking reactions of random-coiled synthetic polymers into defined structures, *e.g.*, cyclic polymers,[1-5] cage-shaped polymers,[6-10] and single-chain nanoparticles (SCNPs),[11-18] have attracted significant interest. Among these unique single-chain technologies, the intramolecular crosslinking of linear polymers bearing crosslinkable functionalities along the main chain to generate a three-dimensional SCNP had been widely studied, aiming at creating functional nanomaterials, such as catalysts,[19-23] nanocarriers,[24-27] and stimuli-responsive sensors.[28-31]
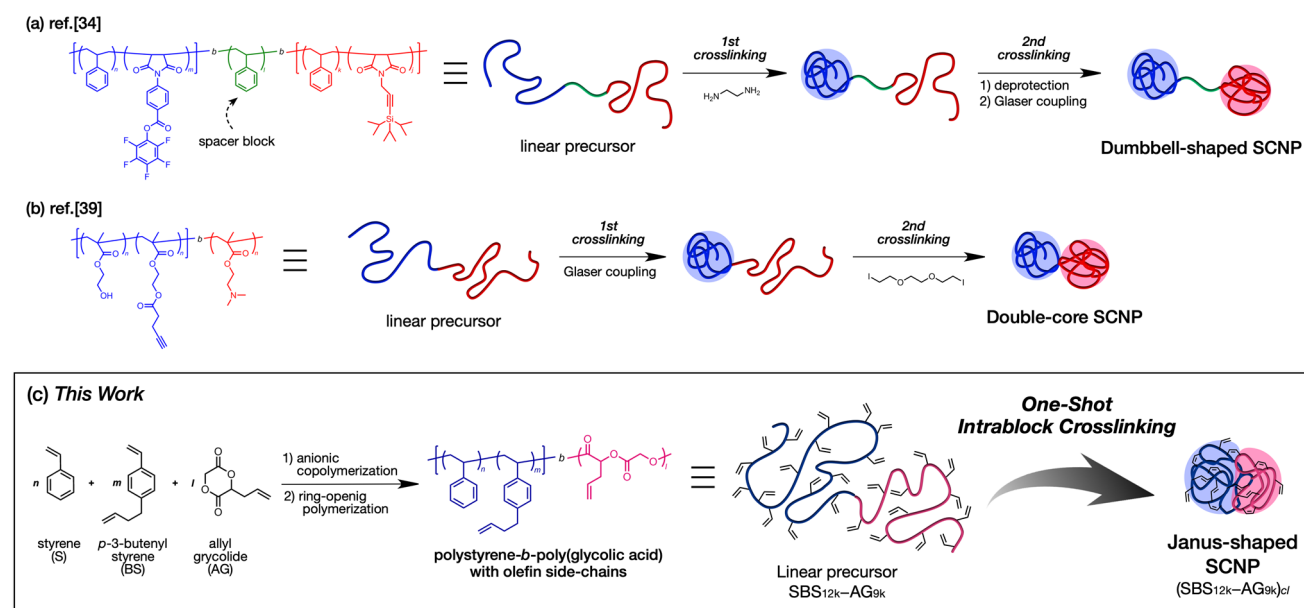
Figure 1. Schematic illustrations for the synthesis of compartmentalized SCNPs. Previous reports regarding the synthesis of (a) dumbbell-shaped and (b) double-core SCNPs. (c) This work: synthesis of Janus-shaped SCNP ((SBS$_{12k}$–AG$_{9k}$)$_{cl}$) via one-shot intrablock crosslinking of linear prepolymer (SBS$_{12k}$–AG$_{9k}$).
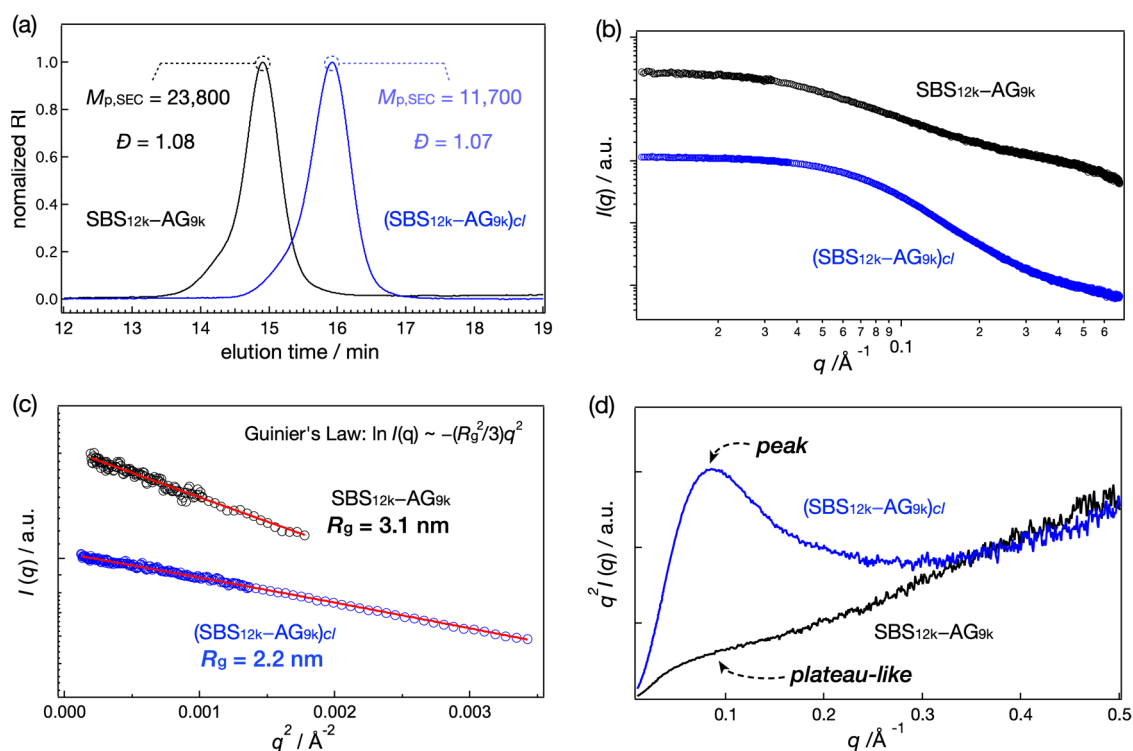
Figure 2. Structural analysis of (SBS$_{12k}$–AG$_{9k}$)$_{cl}$. (a) SEC traces (eluent, THF; flow rate, 1.0 mL min^{-1}) of SBS$_{12k}$–AG$_{9k}$ (black) and (SBS$_{12k}$–AG$_{9k}$)$_{cl}$ (blue). (b) SAXS profiles of SBS$_{12k}$–AG$_{9k}$ (black) and (SBS$_{12k}$–AG$_{9k}$)$_{cl}$ (blue) in DMF (3.0 wt%). (c) Guinier plots and (d) Kratky plots of SBS$_{12k}$–AG$_{9k}$ (black) and (SBS$_{12k}$–AG$_{9k}$)$_{cl}$ (blue), obtained from corresponding SAXS profiles. R_g values were calculated based on Guinier's law: ln $I(q) \sim -(R_g^2/3)q^2$.

Recent studies on SCNPs have focused particularly on constructing the chemically disparate nanodomains in a SCNP molecule using elaborately designed block copolymer (BCP) precursors, known as "compartmentalization". Since the compartmentalization process is reminiscent of the tertiary structure formation in proteins with multiple functional domains,[32-34] such studies are highly attractive for developing the bio-mimicry systems with precise molecular functions.[35-39] One of the interesting compartmentalized configurations is the dumbbell-shaped SCNP, where the chemically different intramolecularly crosslinked blocks are tethered by a short spacer block (**Figure 1a**).[40-42] Furthermore, Matsumoto et al.[43,44], Jiang et al.[45], Ji et al.[46], and Lang et al.[47] recently succeeded in the distinct intramolecular crosslinking of the two segments of BCPs without the spacer, yielding double-core SCNPs (**Figure 1b**). Interestingly, the double-core SCNP fabricated by Jiang's group was found to self-assemble into nanostructured aggregates with an ultra-small periodicity (~4 nm) under certain solvent conditions, indicating the promising potential of the intramolecularly crosslinked BCPs to generate unusual self-assembled nano-objects.[45] Therefore, extensive studies on the compartmentalized SCNPs not only contribute to the development of the biomimetic synthetic systems, but also potentially provide the undiscovered knowledge and introduce novel visions with regard to the BCP self-assembly. However, previous synthetic protocols involving the introduction of the spacer block, adoption of the two disparate crosslinking chemistries, and/or the iterative crosslinking reactions, give rise to significant synthetic complications, which hamper meaningful progress and practical applications of the compartmentalized SCNPs.

In this study, we performed a one-shot intrablock crosslinking of BCPs bearing one particular crosslinkable functionality along the entire chain, realizing a rapid and facile synthesis of compartmentalized SCNPs. An important hypothesis is that the spatially closer crosslinkable points react primarily, rather than farther ones, even though the polymer chain behaves as a random coil. Recently, Kyoda et al. have examined the cyclization of a periodically positioned tetrafunctional linear polymer in high dilution, revealing that the cyclization preferentially occurred between spatially closer reactive points when all the functionalities exhibit identical chemical reactivity.[48] This report strongly supports our hypothesis, i.e. the intramolecular crosslinking process must be directed by the spatial distance between crosslinkable sites. Under such a condition, the one-shot intramolecular crosslinking must produce SCNPs with two chemically compartmentalized spaces, i.e., Janus-shaped SCNP (**Figure 1c**), due to the preferential intrablock crosslinking. Herein, we demonstrate the one-shot intrablock crosslinking of the linear BCPs possessing the pendant olefin groups via the Ru-catalyzed intramolecular olefin metathesis. The resultant Janus-shaped SCNPs with considerably small chain dimensions were revealed to possess the compartmentalized configuration, and also exhibit interesting self-assembling behavior in both bulk and thin film states.

Results and Discussion

Previously, we established a Ru-catalyzed intramolecular olefin metathesis that is applicable to a wide range of precursors possessing double bonds on the side-chain, owing to the high

reactivity and excellent functional group tolerance of the Grubbs' catalyst.[49-52] To demonstrate the one-shot intramolecular crosslinking using this approach, we designed a polystyrene-*block*-poly(glycolic acid) bearing crosslinkable olefin side chains (accounting for 50% of the monomer units) along both blocks. This BCP was obtained according to the following synthetic procedure: the statistical copolymer of styrene (S) and *p*-3-butenyl styrene (BS) with a hydroxyl group at the chain-end (SBS$_{12k}$–OH; $M_{n,SBS}$ = 12,400) was prepared, then allylglycolide (AG) was polymerized using SBS$_{12k}$–OH as a macroinitiator, yielding the desired BCP abbreviated as SBS$_{12k}$–AG$_{9k}$ ($M_{n,AG}$ = 8,700, weight fraction of SBS block (F_{SBS}) = 0.59) (**Figures S1** and **S2**). Subsequently, SBS$_{12k}$–AG$_{9k}$ was subjected to the one-shot intramolecular olefin metathesis reaction using Grubbs' 2nd generation catalyst (G2) ([G2]$_0$/[BS unit]$_0$ = 0.01) under highly diluted conditions ([SBS$_{12k}$–AG$_{9k}$]$_0$ = 0.30 g L^{-1}), yielding the corresponding intramolecularly crosslinked product, *i.e.*, (SBS$_{12k}$–AG$_{9k}$)$_{cl}$, with the olefin conversion (conv.$_{olefin}$) of approximately 85%, as revealed by ^{1}H nuclear magnetic resonance (NMR) and infrared (IR) spectroscopies (**Figures 3a,d** and **S3**). The chain compaction upon intramolecular crosslinking was successfully verified by size exclusion chromatography (SEC) and SEC with multi-angle light scattering and viscosity detectors (SEC-MALLS-Visco). The SEC peak-top molecular weight of (SBS$_{12k}$–AG$_{9k}$)$_{cl}$ ($M_{p,SEC}$ = 11,700) was significantly smaller than that of the linear SBS$_{12k}$–AG$_{9k}$ ($M_{p,SEC}$ = 23,800) (**Figure 2a**), indicating a remarkable reduction in the hydrodynamic volume, which was further supported by the decrease in the intrinsic viscosity ([η]), as determined by SEC-MALLS-Visco (**Table S1**). It is particularly notable that the SEC trace of (SBS$_{12k}$–AG$_{9k}$)$_{cl}$ exhibited a monomodal peak, while maintaining the narrow *Đ* value despite the high olefin conversion, and the absolute weight-averaged molecular weights determined by MALLS ($M_{w,MALLS}$: determined by SEC-MALLS-Visco) were comparable before (22,800) and after the reaction (21,500). These two facts confirm the success in intramolecular crosslinking without unwanted side-reactions,

such as the intermolecular coupling and chain scission.[49]

To further discuss the size and conformation of (SBS$_{12k}$–AG$_{9k}$)$_{cl}$, small-angle X-ray scattering (SAXS) profiles were measured in the diluted DMF solution (3 wt%) using the synchrotron radiation (**Figure 2b**), which were converted to the Guinier (log $I(q)$ *vs.* q^2, where $I(q)$ and q denote the scattered X-ray intensity and scattering vector, respectively; **Figure 2c**) and Kratky plots ($q^2I(q)$ *vs. q*, **Figure 2d**). By analyzing Guinier plots (see Supporting Information for the details), the radius of gyrations (R_gs) of SBS$_{12k}$–AG$_{9k}$ and (SBS$_{12k}$–AG$_{9k}$)$_{cl}$ were estimated to be 3.1 and 2.2 nm, respectively, which again confirmed the remarkable reduction in the chain volume. Moreover, the Kratky plot ($q^2I(q)$ *vs. q*) of the linear SBS$_{12k}$–AG$_{9k}$ exhibited a plateau-like region at 0.10 Å^{-1} < q < 0.20 Å^{-1} whereas that of the (SBS$_{12k}$–AG$_{9k}$)$_{cl}$ obviously showed a characteristic peak at around q = 0.1 Å^{-1}. The difference in the shape of the Kratky plots strongly suggests the transformation of the chain conformation from the unfolded random coil to the folded globule-like state upon intramolecular crosslinking.[10,53] All these results clearly revealed that the intramolecular crosslinking of the SBS$_{12k}$–AG$_{9k}$ successfully fabricated the SCNP ((SBS$_{12k}$–AG$_{9k}$)$_{cl}$) with a significantly compact chain conformation.

To fully understand the compartmentalized structure of (SBS$_{12k}$–AG$_{9k}$)$_{cl}$ and assess the validity of our hypothesis, it is beneficial to compare it with a double-core counterpart that has no interblock crosslinking. For this purpose, the tadpole-shaped and double-core BCPs comprising the same block constituents, *i.e.*, h(SBS$_{12k}$)$_{cl}$–AG$_{11k}$ and h(SBS$_{12k}$)$_{cl}$–(AG$_{11k}$)$_{cl}$, respectively, were synthesized by employing the polymerization–crosslinking–polymerization–crosslinking iterative protocol, as shown in **Scheme S1**. First, SBS$_{12k}$–OH was subjected to intramolecular crosslinking under the previously given conditions, giving the (SBS$_{12k}$)$_{cl}$–OH (conv.$_{olefin}$ = 96%). To avoid possible unwanted crosslinking between the olefins on the SBS(*cl*) block and AG blocks in the final step, the unreacted terminal olefin and newly formed internal olefin were hydrogenated via the diimide reduction (see Supporting
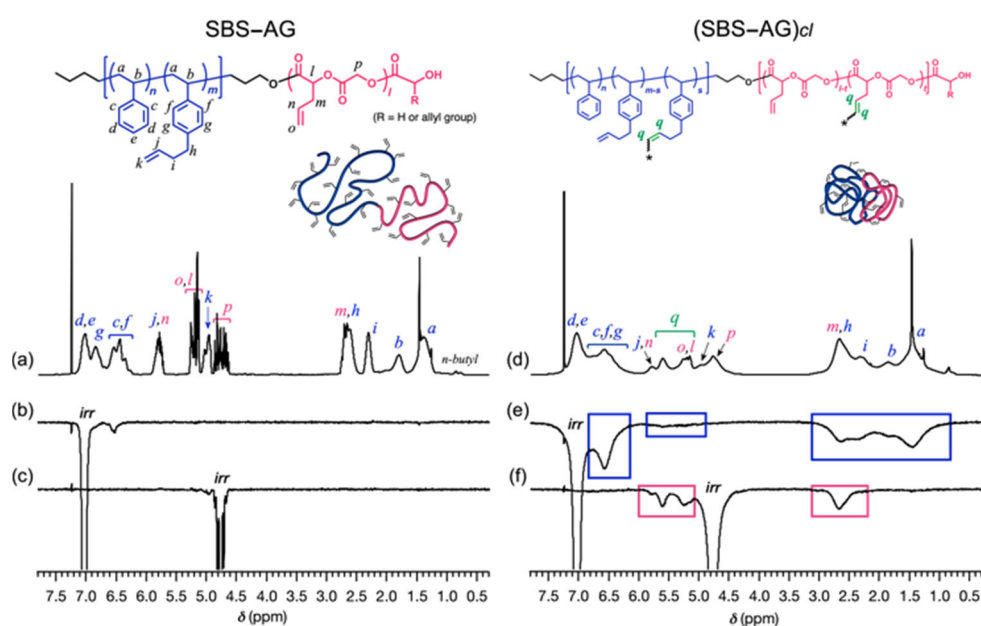
Figure 3. (a)(d) ^{1}H NMR and (b)(c)(e)(f) ^{1}H NOE difference spectra of SBS$_{12k}$–AG$_{9k}$ and (SBS$_{12k}$–AG$_{9k}$)$_{cl}$ in CDCl$_3$ at 50 °C (400 MHz). ^{1}H NOE difference spectra were obtained by irradiating the (b)(e) *d,e* and (c)(f) *p* protons. Colored squares depict ^{1}H NOE signals.

Information), leading to the hydrogenated $(SBS_{12k})_{cl}$–OH, *i.e.*, $h(SBS_{12k})_{cl}$–OH.[54] The obtained $h(SBS_{12k})_{cl}$–OH was then used as a macroinitiator for the subsequent polymerization of AG to provide the tadpole-shaped $h(SBS_{12k})_{cl}$–AG_{11k} ($M_{n,AG}$ = 11,000, F_{SBS} = 0.53). Finally, the intramolecular crosslinking of the AG block was carried out, yielding the double-core $h(SBS_{12k})_{cl}$–$(AG_{11k})_{cl}$ (conv.$_{olefin}$ = 91%). The ^{1}H NMR spectra, SEC traces, and FT-IR spectra are presented in the Supporting Information (**Figures S4-9**). Notably, the iterative synthesis was arguably time-consuming and resulted in considerably quite low product yield (~10% in total). This fact again confirms the advantage of the presented one-shot protocol.

Subsequently, we investigated the localization of each block in such a tightly crosslinked and compactly folded $(SBS_{12k}$–$AG_{9k})_{cl}$ molecule, as well as in the $h(SBS_{12k})_{cl}$–AG_{11k} and $h(SBS_{12k})_{cl}$–$(AG_{11k})_{cl}$ to evaluate the validity of our hypothesis: the two blocks must be compartmentalized in the product obtained by the one-shot intrablock crosslinking. To address this issue, we employed ^{1}H nuclear Overhauser effect (NOE) difference spectroscopy, which yields information about the average local distance between certain protons.[55] **Figures 3** and **S9** show the ^{1}H NOE difference spectra of the samples obtained by irradiating the *d,e*, and *p* protons in the SBS and AG blocks, respectively, as well as the corresponding ^{1}H NMR spectra. In general, the intensity of ^{1}H NOE signals reflects the distance between a proton and the irradiated proton.[56] No significant enhancement in the ^{1}H NOE signals was confirmed for the linear SBS_{12k}–AG_{9k} in both irradiation cases, which is typical for linear random coil polymers (**Figure 3b,c**).[43] On the contrary, the ^{1}H NOE difference spectra of the tadpole $h(SBS_{12k})_{cl}$–AG_{11k} showed strong signals only within the crosslinked $h(SBS)_{cl}$ block upon irradiation of *d,e* protons (see colored squares in **Figure S9b,c**). This result clearly suggests that the protons within the $h(SBS)_{cl}$ block are constrained in a spatially close zone upon intramolecular crosslinking. In the same consequence, the double-core $h(SBS_{12k})_{cl}$–$(AG_{11k})_{cl}$ showed ^{1}H NOE signal enhancement within each block (**Figure S9e,f**). Importantly, because the two blocks of the $h(SBS_{12k})_{cl}$–$(AG_{11k})_{cl}$ are arguably spatially separated in a molecule as a consequence of the iterative synthesis, there is no observable ^{1}H NOE signals corresponding to the interaction of the protons between the block segments. Strikingly, the ^{1}H NOE difference spectra of $(SBS_{12k}$–$AG_{9k})_{cl}$ exhibited quite similar signals with those of the dumbbell-shaped $hSBS_{12k}(cl)$–$AG_{11k}(cl)$ (**Figure 3e,f**): the NOE signals were distinctly enhanced in the SBS and AG blocks, while there are no signals corresponding to the interaction of the protons between the blocks. This represents clear evidence that the SBS and AG blocks were localized at the separated compartments in the intramolecularly crosslinked product. Assuming that the olefin metathesis reaction occurred randomly along the SBS_{12k}–AG_{9k} by the one-shot crosslinking, ^{1}H NOE signals must be observed for all protons in the BCP molecule, irrespective to the block segment. Thus, the above discovery strongly suggests that the crosslinking reaction takes place from spatially closer olefin pairs within each block, and eventually results in block compartmentalization. Because the architecture of $(SBS_{12k}$–$AG_{9k})_{cl}$, including the folded, compact, and chemically compartmentalized structure, is reminiscent of the Janus particles consisting of two disparate components,[57,58] this unique nano-object must be labeled as Janus-shaped SCNP.

To verify the versatility of one-shot intrablock crosslinking, we employed the presented protocol to several different liner precursor BCPs, which can be synthesized by ring-opening polymerization using the SBS-OH macroinitiator: 1) SBS-*block*-poly(2-allyl-*ε*-caprolactone) $(SBS_{22k}$–$2ACL_{30k})$, 2) SBS-*block*-poly(6-allyl-*ε*-caprolactone) $(SBS_{12k}$–$6ACL_{22k})$, 3) SBS-*block*-poly(1,2-epoxy-5-hexane) $(SBS_{12k}$–$EH_{2k})$, and 4) SBS-*block*-poly(9-decenyl grycidyl ether) $(SBS_{12k}$–$DEGE_{8k})$. Note that these BCPs were designed to differ in the main-chain structure, the molecular weight (block composition), and/or the side-chain length from the original SBS_{12k}–AG_{9k}, which allows us to examine the applicable scope. The intramolecular crosslinking of SBS_{22k}–$2ACL_{30k}$, SBS_{12k}–$6ACL_{22k}$, and SBS_{12k}–EH_{2k} were successful, as confirmed by ^{1}H NMR, IR, SEC, and SEC-MALLS-Visco (**Figures 4, S10–S18**, and **Table S2**). In contrast, the multimerized product was obtained from SBS_{12k}–$DEGE_{8k}$. Considering that the intramolecular crosslinking of SBS_{12k}–EH_{2k} with the same polyether main-chain structure proceeded without the multimerized product, the long side chain of DEGE seems to promote the intermolecular coupling (see SEC trace after the reaction). Importantly, the NOE difference spectra of $(SBS_{22k}$–$2ACL_{30k})_{cl}$, $(SBS_{12k}$–$6ACL_{22k})_{cl}$, and $(SBS_{12k}$–$EH_{2k})_{cl}$ clearly indicated block compartmentalization, demonstrating the versatility of the one-shot intrablock crosslinking approach (**Figures 4a-c, S18**). In contrast, NOE signals were enhanced between the blocks as well as within them for the multimerized product of SBS_{12k}–$DEGE_{8k}$ $(m(SBS_{12k}$–$DEGE_{8k})_{cl})$ (**Figure 4d**). Because the olefin metathesis reaction proceeds regardless of the spatial proximity of the double bonds in the case of the intermolecular reaction, the crosslink formation seemed to occur without distinction between and within blocks. The NOE result for the uncompartmentalized crosslinked BCP, in which the two blocks are located at the spatially close zone, unexpectedly
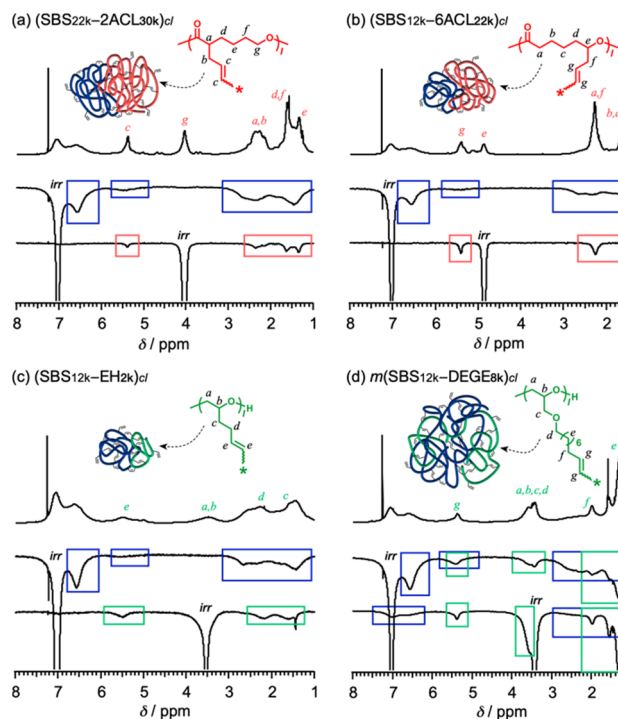
Figure 4. [1]H NOE difference spectra of (a) $(SBS_{22k}$–$2ACL_{30k})_{cl}$, (b) $(SBS_{12k}$–$6ACL_{22k})_{cl}$, (c) $(SBS_{12k}$–$EH_{2k})_{cl}$, and (d) $m(SBS_{12k}$–$DEGE_{8k})_{cl}$ in CDCl$_3$ at 50 °C (400 MHz). The signal assignment of the SBS block is presented in Figure 3. Colored squares indicate ^{1}H NOE signals.

validates the interpretation of the NOE results for the compartmentalized $(SBS_{12k}–AG_{9k})_{cl}$, $(SBS_{22k}–2ACL_{30k})_{cl}$, $(SBS_{12k}–6ACL_{22k})_{cl}$, and $(SBS_{12k}–AGE_{2k})_{cl}$.

One of the most significant characteristics of BCPs is their self-assembling behavior to produce nano-sized microphase-separated structures in the bulk and thin film states.[59-64] Here, we expect the Janus-shaped SCNP to produce the self-assembled nanostructure with a considerably small feature size compared to its linear precursor, owing to compact chain dimensions and block compartmentalization. Thus, we investigated the microphase-separated structures of Janus-shaped $(SBS_{12k}–AG_{9k})_{cl}$ as well as the linear $SBS_{12k}–AG_{9k}$ in the bulk by SAXS experiments. Because the T_g for each block of Janus $(SBS_{12k}–AG_{9k})_{cl}$ was found to be considerably high (**Figure S19**), the solvent vapor annealing (THF, 10 h) was employed to promote self-assembly, while avoiding unwanted side reactions by heating. **Figure 5a** shows the SAXS profile of linear $SBS_{12k}–AG_{9k}$ exhibiting a principal scattering peak at q^* of 0.262 nm^{-1} as well as higher-ordered scattering peaks at the relative q-values of $2:\sqrt{7}$, indicative of a hexagonally close-packed cylindrical (HEX) nanostructure with a domain spacing (d) of 24.0 nm ($d = 2\pi/q^*$).[65] The transmission electron microscope (TEM) images also verified the HEX structure (**Figure S20**). For the Janus-shaped $(SBS_{12k}–AG_{9k})_{cl}$, although the scattering peaks are broader than those for the linear one, two scattering peaks with relative q-values of $1:2$ were observed in the SAXS profile, indicating the formation of a periodic microphase-separated structure (**Figure 5b**). The ability of the Janus-shaped $(SBS_{12k}–AG_{9k})_{cl}$ to produce an ordered nanostructure supports the separated localization of the two blocks in the BCP molecule. The TEM images showed striped patterns in which bright and dark lines were alternately stacked (**Figure S21**), implying the lamellar (LAM) structure formation. Because both of the block chains are not allowed to stretch normal to the domain interface, $(SBS_{12k}–AG_{9k})_{cl}$ needed to form a morphology with lower curvature (e.g. LAM structure) to effectively reduce the interfacial free energy, so that the microphase-separated morphology shifted from HEX to LAM upon the intramolecular crosslinking.[52] As expected, the Janus-shaped $(SBS_{12k}–AG_{9k})_{cl}$ generated the nanostructure with a remarkably small feature size ($d = 12.7$ nm, $q^* = 0.493$ nm^{-1}),
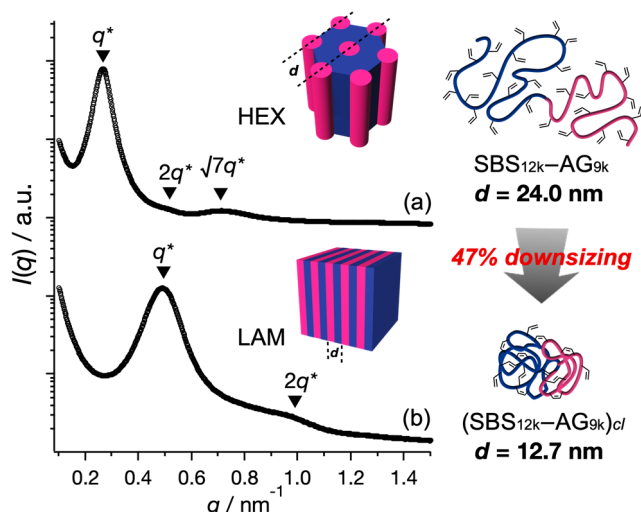
which coincides with a 47% reduction of the d value from the linear precursor. Although a similar conception to downsize the microphase-separated structures is achieved using monocyclic BCPs, the d reduction with respect to the linear counterpart was limited up to 33%.[66] We recently reported a significant d reduction of >50% using bicyclic BCPs; however, their synthesis requires a multistep reaction sequence.[67] To the best of our knowledge, this is the first study to achieve the drastic downscaling by a facile one-shot crosslinking protocol.

The self-assembling behaviors in the thin film were also investigated by the grazing incidence SAXS (GISAXS) experiments using the synchrotron radiation. The thin film samples were prepared by spin-coating the polymer solution (1.0 wt% in toluene, 2000 rpm for 1 min) onto a silicon substrate, followed by annealing with THF vapor (5 h). The GISAXS images of both the linear $SBS_{12k}–AG_{9k}$ and Janus-shaped $(SBS_{12k}–AG_{9k})_{cl}$ films showed the reflection spots along the in-plane direction of thin films (**Figure S22a,c**), as confirmed by the peaks in the in-plane scattering profiles extracted along the $2\theta_f$ direction (**Figure S22b,d**). Although the morphology could not be determined due to the absence of the higher-ordered scattering spots, the significant reduction in the d-values (56% reduction; $SBS_{12k}–AG_{9k}$: 27.0 nm $\rightarrow$ $(SBS_{12k}–AG_{9k})_{cl}$: 12.0 nm) was also verified in the thin film state.

Downsizing the BCP self-assembling nanostructures has been considered as one of the important practical issues to satisfy the ever-increasing demand of miniaturization of integrated circuits using the lithographic technique, i.e., the so-called BCP lithography.[68-73] Although the dimensions of nanostructures could be decreased by simply reducing the degree of polymerization (N) of the BCP with appropriate block pairs, the molecular-weight-dependent material properties, such as mechanical strength and thermal stability, which are crucial factors for the processability, are simultaneously deteriorated. Another problem is that χN (where χ stands for the Flory-Huggins interaction parameter between chemically different monomers) must exceed a critical value for to microphase separation occur, which means that the reduction in N has in principle certain limitations. In this regard, the total molecular weight of the Janus-shaped $(SBS_{12k}–AG_{9k})_{cl}$ is virtually identical to that of its precursor, suggesting that the ultrafine nanostructures could be achieved without deteriorating the molecular-weight-dependent material properties and breaking the χN rule.

Conclusion

In summary, we successfully demonstrated the synthesis of the Janus-shaped SCNPs with the unprecedented, compartmentalized configuration by one-shot intrablock crosslinking of the linear BCPs, bearing the crosslinkable sites along the whole chain. The detailed structural characterizations in solution state clearly revealed not only the folded and compact conformation, but also the compartmentalized block localization of the Janus-shaped SCNPs. The generation of this unique product is presumably related to the higher reactivity of the spatially closer crosslinkers compared to the farther ones. Importantly, the microphase-separated structure of the Janus-shaped $(SBS–AG)_{cl}$ was found to be 47% smaller, as compared to that of the linear SBS–AG precursor, indicating the potential of

Figure 5. Bulk SAXS profiles of (a) linear $SBS_{12k}–AG_{9k}$ and (b) Janus $(SBS_{12k}–AG_{9k})_{cl}$.

the one-shot intrablock crosslinking to contribute to the ultrahigh resolution BCP lithography technology. The presented compartmentalization protocol of one-shot intrablock crosslinking offers novel perspectives in the single-chain technology field, facilitating the advancement of biomimetic polymer chemistries and related material sciences.

[1] H. R. Kiricheldorf, *J. Polym. Sci. Part A: Polym. Chem.* **2010**, *48*, 251–284.

[2] Z. Jia, M. J. Monteiro, *Polym. Sci. Part A: Polym. Chem.* **2012**, *50*, 2085–2097.

[3] D. E. Lonsdale, M. J. Monteiro, *Polym. Sci. Part A: Polym. Chem.* **2011**, *49*, 4603–4612.

[4] T. Yamamoto, S. Yagyu, Y. Tezuka, *J. Am. Chem. Soc.* **2016**, *138*, 3904–3911.

[5] Y. Satoh, H. Matsuno, T. Yamamoto, K. Tajima, T. Isono, T. Satoh, *Macromolecules* **2017**, *50*, 97–106.

[6] Y. Tezuka, A. Tsuchitani, H. Oike, *Macromolecules* **2003**, *36*, 65–70.

[7] J. Jeong, K. Kim, R. Lee, S. Lee, H. Kim, H. Jung, M. A. Kadir, Y. Jang, H. B. Jeon, K. Matyjaszewski, et al., *Macromolecules* **2014**, *47*, 3791–3796.

[8] Y. Mato, K. Honda, K. Tajima, T. Yamamoto, T. Isono, T. Satoh, *Chem. Sci.* **2019**, *10*, 440–446.

[9] M. Gauthier-Jaques, P. Theato, *ACS Macro Lett.* **2020**, *9*, 700–705.

[10] T. Noda, Y. Doi, Y. Ohta, S. ichi Takata, A. Takano, Y. Matsushita, *J. Polym. Sci.* **2020**, *58*, 2098–2107.

[11] C. K. Lyon, A. Prasher, A. M. Hanlon, B. T. Tuten, C. A. Tooley, P. G. Frank, E. B. Berda, *Polym. Chem.* **2015**, *6*, 181–197.

[12] S. Mavila, O. Eivgi, I. Berkovich, N. G. Lemcoff, *Chem. Rev.* **2016**, *116*, 878–961.

[13] E. Harth, B. Van Horn, V. Y. Lee, D. S. Germack, C. P. Gonzales, R. D. Miller, C. J. Hawker, *J. Am. Chem. Soc.* **2002**, *124*, 8653–8660.

[14] N. Hosono, M. A. J. Gillissen, Y. Li, S. S. Sheiko, A. R. A. Palmans, E. W. Meijer, *J. Am. Chem. Soc.* **2013**, *135*, 501–510.

[15] I. Perez-Baena, I. Asenjo-Sanz, A. Arbe, A. J. Moreno, F. Lo Verso, J. Colmenero, J. A. Pomposo, *Macromolecules* **2014**, *47*, 8270–8280.

[16] R. Chen, E. B. Berda, *ACS Macro Lett.* **2020**, *9*, 1836–1843.

[17] H. Frisch, B. T. Tuten, C. Barner-Kowollik, *Israel J. Chem.* **2020**, *60*, 86-99.

[18] J. A. Pomposo, "*Single-Chain Polymer Nanoparticles: Synthesis, Characterization, Simulations, and Applications*" Wiley-VCH (**2017**).

[19] Y. Liu, S. Pujals, P. J. M. Stals, T. Paulöhrl, S. I. Presolski, E. W. Meijer, L. Albertazzi, A. R. A. Palmans, *J. Am. Chem. Soc.* **2018**, *140*, 3423–3433.

[20] H. Rothfuss, N. D. Knöfel, P. W. Roesky, C. Barner-Kowollik, *J. Am. Chem. Soc.* **2018**, *140*, 5875–5881.

[21] Y. Bai, X. Feng, H. Xing, Y. Xu, B. K. Kim, N. Baig, T. Zhou, A. A. Gewirth, Y. Lu, E. Oldfield, et al., *J. Am. Chem. Soc.* **2016**, *138*, 11077–11080.

[22] T. Terashima, *J. Oleo Sci.* **2020**, *69*, 529-538.

[23] J. Chen, E. S. Garcia, S. C. Zimmerman, *Acc. Chem. Res.* **2020**, *53*, 1244-1256.

[24] A. Sanchez-Sanchez, S. Akbari, A. J. Moreno, F. Lo Verso, A. Arbe, J. Colmenero, J. A. Pomposo, *Macromol. Rapid Commun.* **2013**, *34*, 1681–1686.

[25] Y. Bai, H. Xing, G. A. Vincil, J. Lee, E. J. Henderson, Y. Lu, N. G. Lemcoff, S. C. Zimmerman, *Chem. Sci.* **2014**, *5*, 2862–2868.

[26] C. C. Cheng, F. C. Chang, H. C. Yen, D. J. Lee, C. W. Chiu, Z. Xin, *ACS Macro Lett.* **2015**, *4*, 1184–1188.

[27] E. Verde-Sesto, A. Arbe, A. J. Moreno, D. Cangialosi, A. Alegría, J. Colmenero, J. A. Pomposo, *Mater. Horiz.* **2020**, *7*, 2292-2313.

[28] M. A. J. Gillissen, I. K. Voets, E. W. Meijer, A. R. A. Palmans, *Polym. Chem.* **2012**, *3*, 3166–3174.

[29] L. Delafresnaye, N. Zaquen, R. P. Kuchel, J. P. Blinco, P. B. Zetterlund, C. Barner-Kowollik, *Adv. Funct. Mater.* **2018**, *28*, 1800342.

[30] C. Heiler, S. Bastian, P. Lederhose, J. P. Blinco, E. Blasco, C. Barner-Kowollik, *Chem. Commun.* **2018**, *54*, 3476–3479.

[31] J. Steinkoenig, M. M. Zieger, H. Mutlu, C. Barner-Kowollik, *Macromolecules* **2017**, *50*, 5385–5391.

[32] C.-J. Tsai, S. Kumar, B. Ma, R. Nussinov, *Protein Sci.* **1999**, *8*, 1181–1190.

[33] J. Markl, *Biochim. Biophys. Acta* **2013**, *1834*, 1840–1852.

[34] C. M. Dobson, *Nature* **2003**, *426*, 884–890.

[35] S. F. M. van Dongen, H.-P. M. de Hoog, R. J. R. W. Peters, M. Nallani, R. J. M. Nolte, J. C. M. van Hest, **2009**, *109*, 6212–6274.

[36] Z. Li, E. Kesselman, Y. Talmon, M. A. Hillmyer, T. P. Lodge, *Science* **2004**, *306*, 98–101.

[37] R. Chandrawati, M. P. Van Koeverden, H. Lomas, F. Caruso, *J. Phys. Chem. Lett.* **2011**, *2*, 2639–2649.

[38] A. H. Gröschel, F. H. Schacher, H. Schmalz, O. V. Borisov, E. B. Zhulina, A. Walther, A. H. E. Müller, *Nat. Commun.* **2012**, *3*, DOI 10.1038/ncomms1707.

[39] A. Belluati, S. Thamboo, A. Najer, V. Maffeis, C. von Planta, I. Craciun, C. G. Palivan, W. Meier, *Adv. Funct. Mater.* **2020**, *30*, DOI 10.1002/adfm.202002949.

[40] R. K. Roy, J. F. Lutz, *J. Am. Chem. Soc.* **2014**, *136*, 12888–12891.

[41] Z. Cui, L. Huang, Y. Ding, X. Zhu, X. Lu, Y. Cai, *ACS Macro Lett.* **2018**, *7*, 572–575.

[42] Z. Cui, H. Cao, Y. Ding, P. Gao, X. Lu, Y. Cai, *Polym. Chem.* **2017**, *8*, 3755–3763.

[43] M. Matsumoto, T. Terashima, K. Matsumoto, M. Takenaka, M. Sawamoto, *J. Am. Chem. Soc.* **2017**, *139*, 7164–7167.

[44] M. Matsumoto, M. Sawamoto, T. Terashima, *ACS Macro Lett.* **2019**, *8*, 320–325.

[45] L. Jiang, M. Xie, J. Dou, H. Li, X. Huang, D. Chen, *ACS Macro Lett.* **2018**, *7*, 1278–1282.

[46] X. Ji, Y. Zhang, H. Zhao, *Chem. Eur. J.* **2018**, *24*, 3005–3012.

[47] F. Lang, D. Xiang, J. Wang, L. Yang, Z. Yang, *Macromolecules* **2020**, *53*, 2271–2278.

[48] K. Kyoda, T. Yamamoto, Y. Tezuka, *J. Am. Chem. Soc.* **2017**, *141*, 7526–7536.

[49] K. Watanabe, R. Tanaka, K. Takada, M. J. Kim, J. S. Lee, K. Tajima, T. Isono, T. Satoh, *Polym. Chem.* **2016**, *7*, 4782–4792.

[50] R. Tanaka, K. Watanabe, T. Yamamoto, K. Tajima, T. Isono, T. Satoh, *Polym. Chem.* **2017**, *8*, 3647–3656.

[51] K. Watanabe, S. Katsuhara, H. Mamiya, T. Yamamoto, K. Tajima, T. Isono, T. Satoh, *Chem. Sci.* **2019**, *10*, 3330–3339.

[52] K. Watanabe, S. Katsuhara, H. Mamiya, Y. Kawamura, T. Yamamoto, K. Tajima, T. Isono, T. Satoh, *Nanoscale* **2020**, *12*, 16526–16534.

[53] T. Iwamoto, Y. Doi, K. Kinoshita, Y. Ohta, A. Takano, Y. Takahashi, M. Nagao, Y. Matsushita, *Macromolecules* **2018**, *51*, 1539–1548.

[54] S. Kobayashi, L. M. Pitet, M. A. Hillmyer, *J. Am. Chem. Soc.* **2011**, *133*, 5794–5797.

[55] A.-ur-Rahman, M. I. Choudhary, A.-tul-Wahab, *Solving Problems with NMR Spectroscopy (Second Edition)*, **2016**, pp.227–264.

[56] Y. Cheng, Y. Li, Q. Wu, T. Xu, *J. Phys. Chem. B* **2008**, *112*, 12674–12680.

[57] S. Jiang, Q. Chen, M. Tripathy, E. Luijten, K. S. Schweizer, S. Granick, *Adv. Mater.* **2010**, *22*, 1060–1071.

[58] A. Walther, A. H. E. Müller, *Chem. Rev.* **2013**, *113*, 5194–5261.

[59] F. S. Bates, *Annu. Rev. Phys. Chem.* **1990**, *41*, 525–527.

[60] M. W. Matsen, F. S. Bates, *Macromolecules* **1996**, *29*, 7641–7644.

[61] F. S. Bates, G. H. Fredrickson, *Phys. Today* **1999**, *52*, 32–38.

[62] S. B. Darling, *Prog. Polym. Sci.* **2007**, *32*, 1152–1204.

[63] C. Park, J. Yoon, E. L. Thomas, *Polymer* **2003**, *44*, 6725–6760.

[64] J. N. L. Albert, T. H. Epps, *Mater. Today* **2010**, *13*, 24–33.

[65] I. W. Hamley, V. Castelletto, *Small-Angle Scattering of Block Copolymers in the Melt, Solution and Crystal States*, **2004**.

[66] J. E. Poelma, K. Ono, D. Miyajima, T. Aida, K. Satoh, C. J. Hawker, *ACS Nano* **2012**, *6*, 10845–10854.

[67] B. J. Ree, Y. Satoh, T. Isono, T. Satoh, *Nano Lett.* **2020**, *20*, 6520–6525.

[68] J. Bang, U. Jeong, D. Y. Ryu, T. P. Russell, C. J. Hawker, *Adv. Mater.* **2009**, *21*, 4769–4792.

[69] C. M. Bates, M. J. Maher, D. W. Janes, C. J. Ellison, C. G. Willson, *Macromolecules* **2014**, *47*, 2–12.

[70] M. Park, C. Harrison, P. M. Chaikin, R. A. Register, D. H. Adamson, *Science* **1997**, *276*, 1401–1404.

[71] M. P. Stoykovich, P. F. Nealey, *Mater. Today* **2006**, *9*, 20–29.

[72] S. J. Jeong, J. Y. Kim, B. H. Kim, H. S. Moon, S. O. Kim, *Mater. Today* **2013**, *16*, 468–476.

[73] K. Koo, H. Ahn, S. W. Kim, D. Y. Ryu, T. P. Russell, *Soft Matter* **2013**, *9*, 9059–9071.

Entry for the Table of Contents
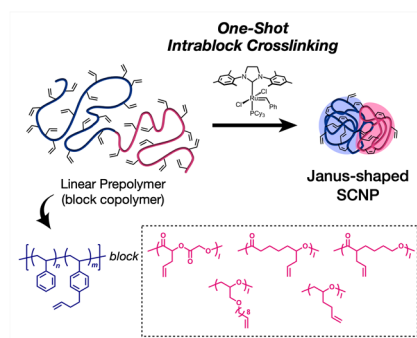
A novel one-shot intrablock crosslinking protocol was demonstrated to achieve a rapid and facile synthesis of single-chain nanoparticles (SCNPs) with two chemically compartmentalized domains (i.e., Janus-shaped SCNPs) from the various diblock copolymers bearing one particular crosslinkable functionality across the entire polymer chain. Additionally, Janus-shaped SCNP was found to produce significantly small microphase-separated structure.